Applied Catalysis B: Environmental 237 (2018) 68–73

Contents lists available at ScienceDirect

Applied Catalysis B: Environmental

journal homepage: www.elsevier.com/locate/apcatb

A rapidly room-temperature-synthesized Cd/ZnS:Cu nanocrystal photocatalyst for highly efficient solar-light-powered CO_2 reduction

Xianguang Meng[a,b,c,**], Guifu Zuo[a,b], Peixiao Zong[a,b], Hong Pang[c,d], Jian Ren[e], Xiongfeng Zeng[a,b], Shanshan Liu[a,b], Yi Shen[a,b], Wei Zhou[f,*], Jinhua Ye[c,d,g,h,**]

[a] Key Laboratory of Environment Functional Materials of Tangshan City, Hebei Provincial Key Laboratory of Inorganic Nonmetallic Materials, College of Materials Science and Engineering, North China University of Science and Technology, Tangshan, 063210, Hebei, PR China
[b] Photo-Functional Materials Research Platform, College of Materials Science and Engineering, North China University of Science and Technology, Tangshan, 063210, PR China
[c] International Center for Materials Nanoarchitectonics (WPI-MANA), National Institute for Materials Science (NIMS), 1-1 Namiki, Tsukuba, Ibaraki, 305-0044, Japan
[d] Graduate School of Chemical Sciences and Engineering, Hokkaido University, Sapporo, 060-0814, Japan
[e] Institute of Methods for Materials Development, Helmholtz-Zentrum Berlin, Albert-Einstein-Strasse 15, 12489, Berlin, Germany
[f] Department of Applied Physics, Tianjin Key Laboratory of Low Dimensional Materials Physics and Preparing Technology, School of Science, Tianjin University, Tianjin, 300072, PR China
[g] TU-NIMS International Collaboration Laboratory, School of Materials Science and Engineering, Tianjin University, 92 Weijin Road, Tianjin, 300072, PR China
[h] Collaborative Innovation Center of Chemical Science and Engineering (Tianjin), Tianjin, 300072, PR China

ARTICLE INFO

Keywords:
Photocatalysis
CO_2 reduction
ZnS
Room-temperature synthesis
DFT calculations

ABSTRACT

An ideal photocatalyst that can promisingly convert CO_2 should have suitable band gap and fully consider the activation of reaction. However, well-designed photocatalytic materials with these aspects are very limited. This study reports a highly efficient CO_2 reduction photocatalyst based on ZnS nanocrystals which can be rapidly synthesized at room temperature and operated under solar light irradiation at all-inorganic reaction system. Two functional elements, Cu and Cd, are respectively used as dopant and cocatalyst of ZnS nanocrystal for selective CO_2 reduction. Cu^+ doping expands the photoabsorption of ZnS into visible light region and the simultaneous Cd^{2+} surface modification significantly improves the activity of CO_2 reduction with 99% formic acid selectivity. A combination of charge density distribution and electronic state studies reveal that the Cd *s* orbital displays obviously higher density of states near band-edge with a relatively lower lying band center than that of Zn *s* orbital. This will greatly favor the charge transfer from conduction band of ZnS to the surface state created by Cd^{2+} for catalyzing CO_2 reduction.

1. Introduction

Solar fuel production from photocatalytic CO_2 reduction represents a promising solution for sustainable energy supply with simultaneously mitigating the environmental impact of greenhouse gas emission. Unfortunately, the performance of most of semiconductor photocatalysts remain far less satisfied in this respect. Due to the harsh requirements from both thermodynamics and kinetics aspects, high conduction band (CB) potential and good activation ability to CO_2 molecules are indispensable. In order to realize appreciable reaction rate of CO_2 photoreduction under visible light, a popular strategy in the recent studies attempts to couple high CB inorganic semiconductors (e.g., TaON and C_3N_4) with organic complexes as photosensitizer/electrocatalyst in the presence of organic reaction medium [1,2]. For such organic environment, firstly, valuable sacrificial organic compounds are generally necessary, which makes the overall CO_2 reduction reaction uneconomical. Secondly, organic matters can also lead to serious interference of CO_2 reduction product identification. Lastly, the functional organic complexes are apt to be deactivated by the photocorrosion of themselves or photo-oxidation of adjacent inorganic semiconductors, impairing their long term reaction durability [3]. Therefore, it remains very much attractive and challenging to develop a photocatalyst that can achieve efficient and stable CO_2 conversion in all-inorganic aqueous reaction medium under mild irradiation input, such as visible light or solar light.

Our previous studies have shown that high CB potential and active

* Corresponding author.
** Corresponding authors at: International Center for Materials Nanoarchitectonics (WPI-MANA), National Institute for Materials Science (NIMS), 1-1 Namiki, Tsukuba, Ibaraki, 305-0044, Japan.
E-mail addresses: mengxg_materchem@163.com (X. Meng), weizhou@tju.edu.cn (W. Zhou), jinhua.ye@nims.go.jp (J. Ye).

https://doi.org/10.1016/j.apcatb.2018.05.066
Received 8 March 2018; Received in revised form 25 April 2018; Accepted 24 May 2018
Available online 24 May 2018
0926-3373/

surface structure enable colloidal ZnS to be a veritably "efficient photocatalyst" for CO_2 conversion [4]. However, the large band gap of colloidal ZnS determined that it can only be operated under UV light. In order to design an exceptionally efficient and solar light active CO_2 reduction photocatalyst, an ideal strategy is to take the advantages of ZnS matrix and further modulate its energy band structure and surface reactivity. Many ZnS based visible light active photocatalysts have been developed previously at the aim of photocatalytic hydrogen evolution reaction (HER), such as ZnS-$CuInS_2$-$AgInS_2$ and ZnS-CdS solid solution systems, and Ni or Pb doped ZnS, etc [5]. For preparing these sulfide photocatalysts, hydrothermal or heat treatment is needed to get high crystallinity. It is widely accepted that semiconductor photocatalysts with high crystallinity generally means a decreased recombination of photo-excited carriers or increased photocatalytic HER activity. However, our recent study verifies that the high crystallinity of ZnS unexpectedly quenched photocatalytic CO_2 reduction due to the lack of intrinsically reactive surface structure, such as S vacancies [4]. Therefore, a CO_2-reduction-oriented ZnS photocatalyst should be more favorably prepared by heating-free procedure to retain its reactive surface structure as much as possible.

Cu doped ZnS (noted as ZnS:Cu for clarity) is a visible light active photocatalyst [6]. HER can proceed over ZnS:Cu in aqueous solution in the absence of noble metal cocatalysts and sulphur ion (S^{2-}) as sacrificial electron donor, only requiring sulfite ion (SO_3^{2-}) as electron donor which can be obtained from the industrial SO_2 exhaust. It is generally considered that the 3*d* orbital of the formed Cu^+ dopant in ZnS:Cu created an electron donor level above a valence band of ZnS [6,7]. Since the doping of Cu narrows the band gap without decreasing CB level, in principal, high reduction potential of ZnS can be retained for potentially efficient CO_2 reduction. Motivated by such speculation, we developed an exceptionally efficient and solar-light-active photocatalyst based on colloidal ZnS for CO_2 reduction in all-inorganic aqueous reaction system. With the simultaneous functionalization of Cu dopant and Cd cocatalyst (noted as Cd/ZnS:Cu for clarity), efficient photocatalytic CO_2 reduction under solar light was realized. Cu^+ doping expanded the photoabsorption of ZnS nanocrystal into visible light region and the simultaneous Cd^{2+} surface modification significantly improved the activity of CO_2 reduction with exceptional formic acid selectivity (see Scheme 1).

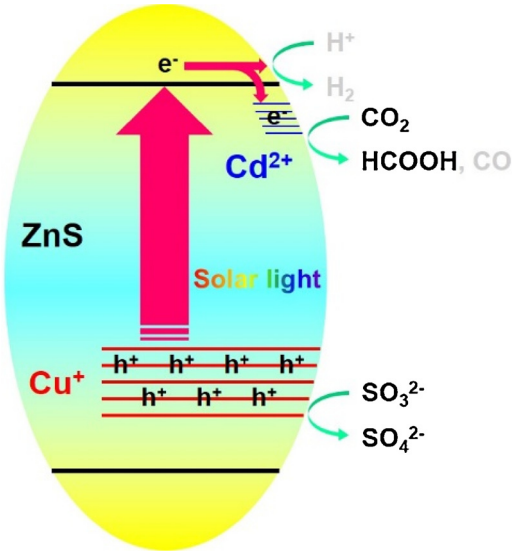

Scheme 1. Design principle of efficient solar light active Cd/ZnS:Cu nanocrystal photocatalyst.

2. Results and discussion

The colloidal ZnS (0.1 g) with different doping molar ratios ([Cu]/([Cu] + [Zn]) = 0%, 0.1%, 0.2%, 0.5%, 2%, and 4%) can be instantly obtained by directly pouring freshly prepared Na_2S solution into solution containing $ZnSO_4$ and $CuSO_4$ under vigorous stirring at room temperature. Without any further heat treatment, the ZnS:Cu was separated by centrifugation (10,000 rpm, 2 min) and redispersed in stirred water (100 mL). If needed, Cd^{2+} cocatalyst can be loaded at this time by quantitatively adding cadmium sulfate solution into the reaction suspension. Afterwards, K_2SO_3 and $KHCO_3$ were dissolved into the reaction suspension with the concentration of 0.1 M and 0.5 M respectively. Finally, the reaction system was evacuated and high-purity CO_2 (99.999%) was injected until the reaction suspension was saturated. The final pressure of CO_2 in the gas space of cell is 101–102 kPa (atmospheric pressure). A solar light simulator was used as the light source. Before activity test, the current of solar light simulator was modulated to an extent where the total output light intensity at reaction solution surface is equal to AM 1.5 (100 mW/cm^2). The irradiation area is 30 cm^2. Detailed methods of sample characterization, product analysis and experiment setup are described in Supporting Information or our previous report [4].

As reported previously, the freshly prepared colloidal ZnS showed an amorphous feature and large band gap (3.8 eV) [4]. Upon continuous stirring during photocatalytic reaction, the colloidal ZnS as well as ZnS:Cu underwent slight crystallization and gradual change in photoabsorption. All these photocatalysts after reaction showed broad diffraction peaks of zinc blende structure in the X ray diffraction (XRD) analysis (Fig. 1a). Meanwhile, the band gap of the undoped colloidal ZnS reduces from 3.8 eV to 3.6 eV (ca. 345 nm, Fig. 1b and c). The colour of ZnS:Cu gradually changed from gray into yellow within a few hours' stirring (Fig. S1). With increasing the doping concentration of Cu, the colloidal photocatalysts exhibit stronger photoabsorption in visible light region (Fig. 1b and c), making enhanced photocatalytic performance possible due to better utilization of solar light. TEM images show that the particles size of ZnS and ZnS:Cu nanocrystals are ca. 5 nm (Fig. S2).

The photocatalytic synthesis gas (CO and H_2 mixture) and formic acid (mainly in the form of formate $HCOO^-$ in the present reaction suspension with pH 7–7.5) production under solar light are closely dependent on the doping amount of Cu in colloidal ZnS (Fig. 2). The optimized doping amount of Cu is 0.2%-0.5%, where both the synthesis gas and formic acid reach their highest production rates. For sulfides, it is supposed that the activation of both proton reduction for HER and CO_2 reduction for CO production are associated with the surface S vacancies [8–10]. As ZnS:Cu inherits the structure of colloidal ZnS, large amount of surface defects, especially S vacancies, can be retained. This is responsible for the high synthesis gas production rate of ZnS:Cu nanocrystals. Moreover, density functional theory (DFT) calculations show that the S vacancy formation energies could be significantly lowered when Cu substitutes Zn in ZnS, as listed in Table S1 (for computational details, see supporting information). This implies that more S vacancies will form at both surface and bulk of ZnS nanocrystal during Cu doping. Closely resembling the scenario of $Zn_{0.5}Cd_{0.5}S$:Cu analogue in our previous report [7], two Cu^+ ions will be produced in ZnS for the reason of charge compensation when one S vacancy forms. Therefore, Cu doping is bifunctional, i.e., narrowing the band gap of ZnS nanocrystals by creating Cu^+ 3*d* energy level (Scheme 1) and increasing reactive S vacancies on ZnS surface for synthesis gas production. A higher Cu doping amount will take adverse effect to the photocatalytic performance possibly because excessive Cu doping has produced too many S vacancies as the recombination centers of photo-excited carriers in ZnS:Cu nanocrystals.

To confirm the carbon source of products, $^{13}CO_2$ was used as reactant in isotope experiment and injected into the reaction system only containing 0.1 M K_2SO_3 and ZnS:0.2% Cu for pre-absorption. $KHCO_3$

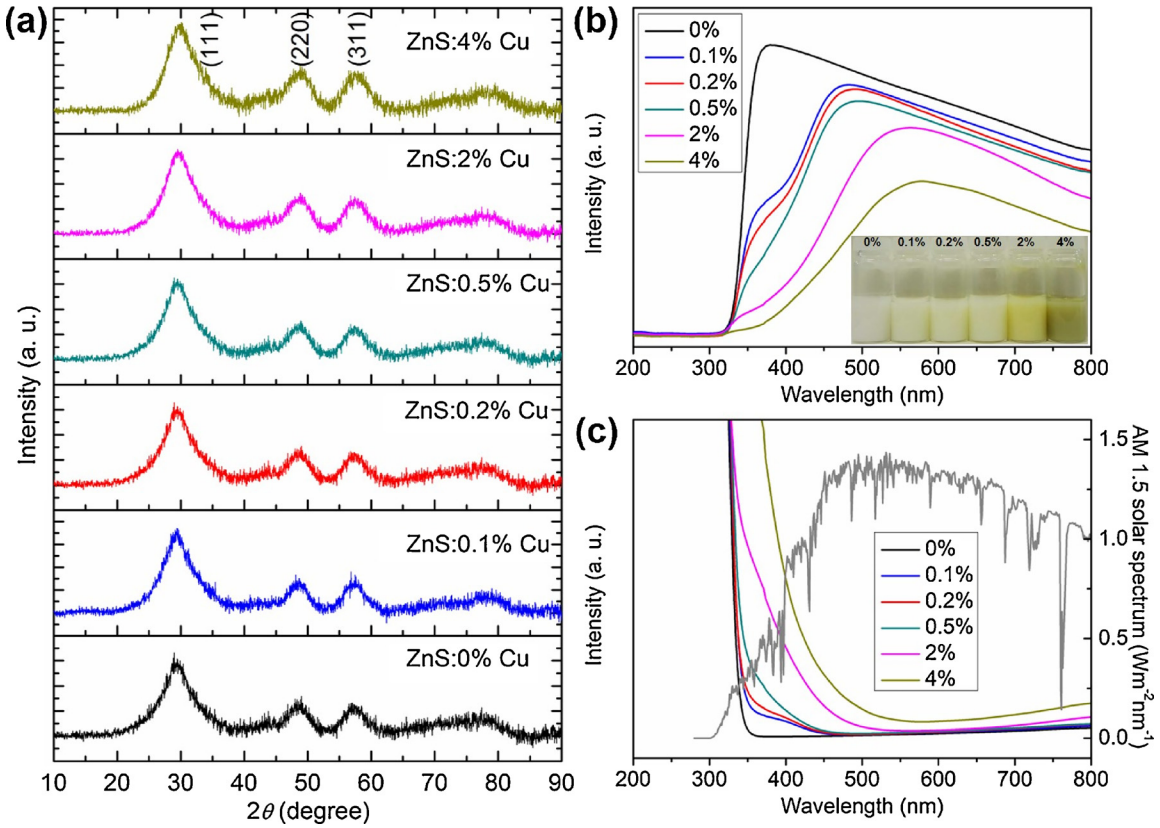

Fig. 1. Characterizations of ZnS and ZnS:Cu nanocrystals in the state of wet gel (i.e., precipitate obtained by centrifugation). (a) XRD patterns. (b) UV-VIS reflection spectra of photocatalysts after reaction. The photographs of photocatalyst suspensions are shown in the inset. (c) The spectral overlap between AM 1.5 and UV-VIS absorption spectra of photocatalysts after KM transformation from (b).

was not added in isotope experiment to maintain the purity of ^{13}C isotope in reaction system. The gas chromatography–mass spectroscopy (GC–MS) result (Fig. 3a) clearly shows the formation of ^{13}CO (m/z = 29). N_2 (m/z = 28) and O_2 (m/z = 32) can be also identified because a little amount of entrained air was inevitable during the transfer of gas sample into GC–MS (see the relation between total ion chromatogram and m/z in Fig. S3). NMR measurements of product at liquid phase show an obvious ^{13}C NMR peak at 170.5 ppm assigned to $H^{13}COO^-$ (Fig. 3b). The ^1H NMR doublet (Fig. 3c) corresponds to the proton that is coupled to the ^{13}C in $H^{13}COO^-$. By contrast, normal HCOOH has only one ^1H NMR peak at ca. 8.3 ppm (Fig. S4). Therefore, both CO and HCOOH are completely derived from CO_2 reduction.

In order to enhance photocatalytic CO_2 conversion, a 2 mol% Cd^{2+} modified ZnS:0.2% Cu photocatalyst was designed (noted as 2% Cd/ZnS:0.2% Cu for clarity). The sample can be readily prepared by quantitatively adding cadmium sulfate solution into the reaction suspension containing colloidal ZnS:0.2% Cu, with the same method reported previously [4]. Cd^{2+} modification remarkably improved the CO_2 reduction for selective HCOOH production with respect to synthesis gas (Fig. 4a–c). The HCOOH production amount of 2% Cd/ZnS:0.2% Cu is 46.7 times higher than ZnS:0.2% Cu. The selectivity of HCOOH over 2% Cd/ZnS:0.2% Cu reaches 99%. The apparent quantum yield (AQY) of HCOOH was measured under monochromatic UV (381.8 nm, $\lambda_{1/2}$ = 24.4 nm) and visible light (417.9 nm, $\lambda_{1/2}$ = 14.4 nm) according to the equition AQY (HCOOH) = N(HCOOH) × 2/N(Photons) × 100%, where N(HCOOH) and N(Photons) signify the number of HCOOH molecules and the number of incident photons, respectively. The AQYs of HCOOH over 2% Cd/ZnS:0.2% Cu are 17.8% (381.8 nm) and 5.8% (417.9 nm), and that over 2% Cd/ZnS:0.5% Cu are 23.3% (381.8 nm) and 13.2% (417.9 nm), indicating that, at the wavelength region longer than the absorption edge of colloidal ZnS (345 nm), the AQY rises when increasing the doping amount of Cu from 0.2% to 0.5%. This also implies that the AQY at the wavelengh shorter than 345 nm should decrease at the same time.

Control experiment shows that the CO_2 reduction performance of 2% Cd/ZnS:0.2% Cu is much superior to the homogeneous 2% Cd^{2+}

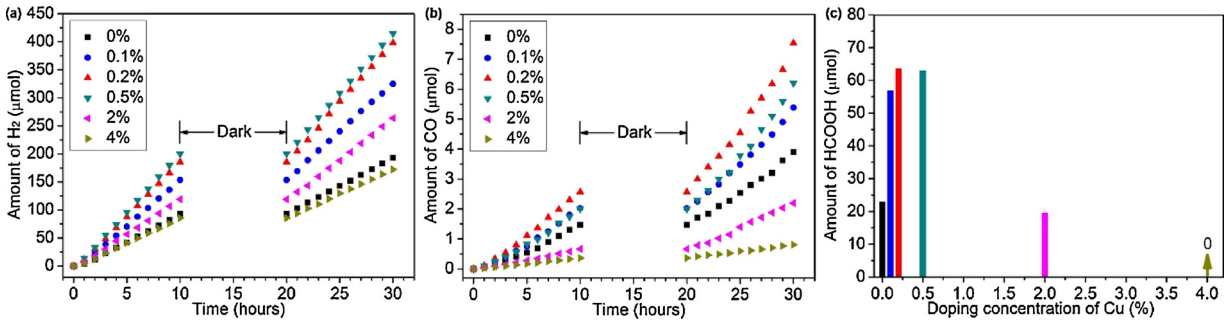

Fig. 2. Time course of photocatalytic (a) H_2 and (b) CO evolution, and (c) HCOOH production after 20 h' solar light irradiation over colloidal ZnS and ZnS:Cu.

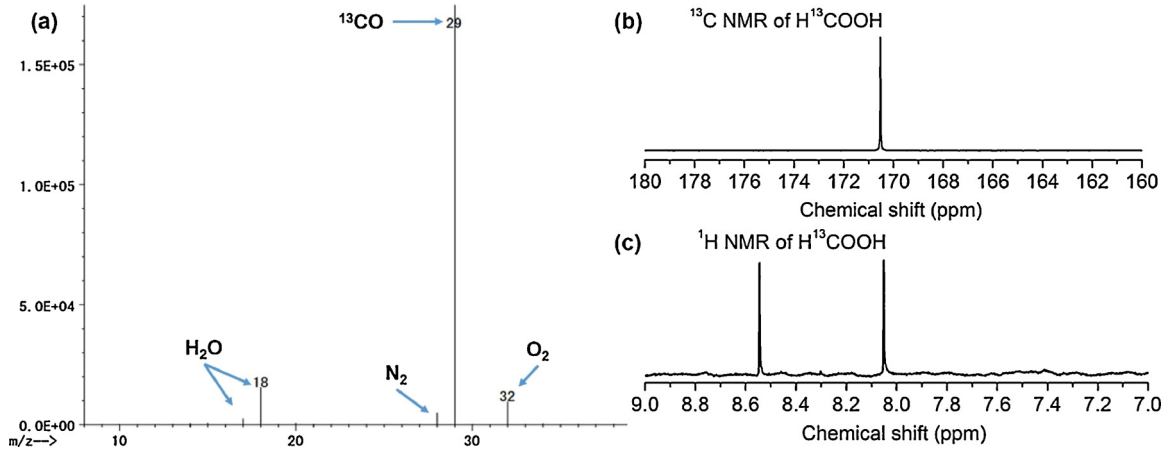

Fig. 3. Mass spectrum of (a) ^{13}CO, (b) ^{13}C NMR and (c) ^{1}H NMR spectra of H^{13}COOH produced in isotope tracing experiment.

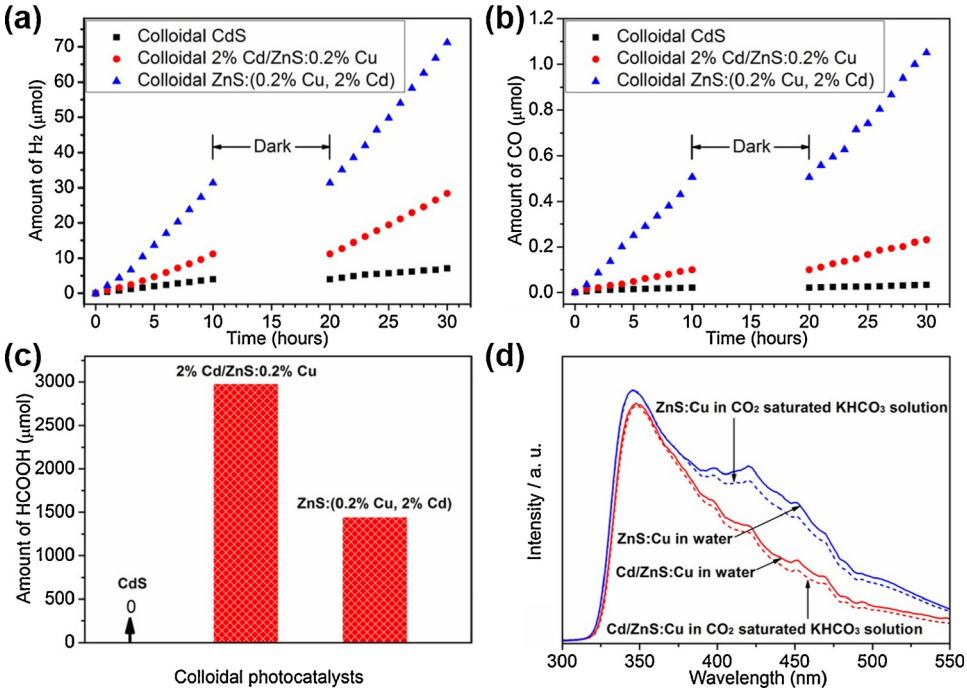

Fig. 4. Time course of photocatalytic (a) H_2, (b) CO evolution, and (c) HCOOH production after 20 h' solar light irradiation over colloidal CdS, 2% Cd/ZnS:0.2% Cu, and ZnS:(0.2% Cu, 2% Cd). (d) Fluorescence spectra of ZnS:0.2% Cu and 2% Cd/ZnS:0.2% Cu in water and CO_2 saturated $KHCO_3$ solution (For interpretation of the references to colour in this figure legend, the reader is referred to the web version of this article).

doped sample, i.e., ZnS:(0.2% Cu, 2% Cd), indicating that Cd^{2+} is more favorably used as cocatalyst through surface modification. Surface modification increases the coverage of Cd^{2+} on the surface of colloidal particles, which leads to the change of the reaction selectivity from HER into CO_2 reduction. Moreover, under present reaction condition, the visible light active colloidal CdS photocatalyst only shows negligible activity for both synthesis gas and HCOOH production, showing that 2% Cd/ZnS:0.2% Cu is a very optimized design. According to the difference of solubility products K_{sp} between CdS ($pK_{sp} \approx 26$) and ZnS ($pK_{sp} \approx 22$), Zn^{2+} at the surface of ZnS nanocrystals will be readily exchanged by Cd^{2+} ion. Although it can be estimated that there are only ca. 16.6 Cd^{2+} ions per ZnS nanocrystal (in 5 nm particle size with 2 mol% Cd^{2+} loading), the fluorescence spectra show that such a few Cd^{2+} ions modification leads to obvious quenching of the broad emission at 380–500 nm resulting from the recombination of photo-excited carries at S vacancies, which can be further quenched in the presence of carbon source (Fig. 4d). Therefore, Cd^{2+} cocatalyst can effectively suppress the recombination of photo-excited carries.

In this work, Cd^{2+} modification on colloidal ZnS:Cu shows similar enhancement effect as Cd^{2+} modified colloidal ZnS in our previous report [4], revealing that Cu doping did not interference the unique function of Cd^{2+} ion as an excellent CO_2 reduction selective cocatalyst. However, the mechanism underlying the superior CO_2 reduction rate over the Cd^{2+} modified nanocrystal photocatalyst is still unclear. For this purpose, the charge densities of Cd^{2+} modified ZnS (111) and (110) planes were computed by DFT method herein (for computational details, see supporting information). Note that (110) plane here is equivalent to (220) plane in above XRD pattern (Fig. 1a). Our results demonstrated remarkably high charge density located at the surface Cd site (Fig. 5a–d), suggesting that the excited electrons in ZnS (or ZnS:Cu) system prefer to be trapped by the surface state created by Cd^{2+}, as the reaction sites of photocatalytic CO_2 reduction. Next, we compared the projected density of states (PDOS) of the Zn atom and Cd atom at ZnS surface and analyzed the contributions from their electronic states of *s*, *p* and *d* orbitals to the photocatalytic CO_2 reduction (Fig. 5e–j). The band-edge electronic states of these orbitals above the Fermi level E_f, i.e., the electronic states near the CB of ZnS (mainly composed of Zn *sp* orbitals), should be of particular interest for understanding the kinetic behavior of photo-excited electrons. The obtained data indicate that, compared with the *p* and *d* orbitals (Fig. 5f, g, i, j), the energy distribution of *s* orbitals for Zn and Cd (Fig. 5e, h) at both crystal surfaces are closer to the E_f. Notably, the Cd *s* orbital above E_f displays obviously

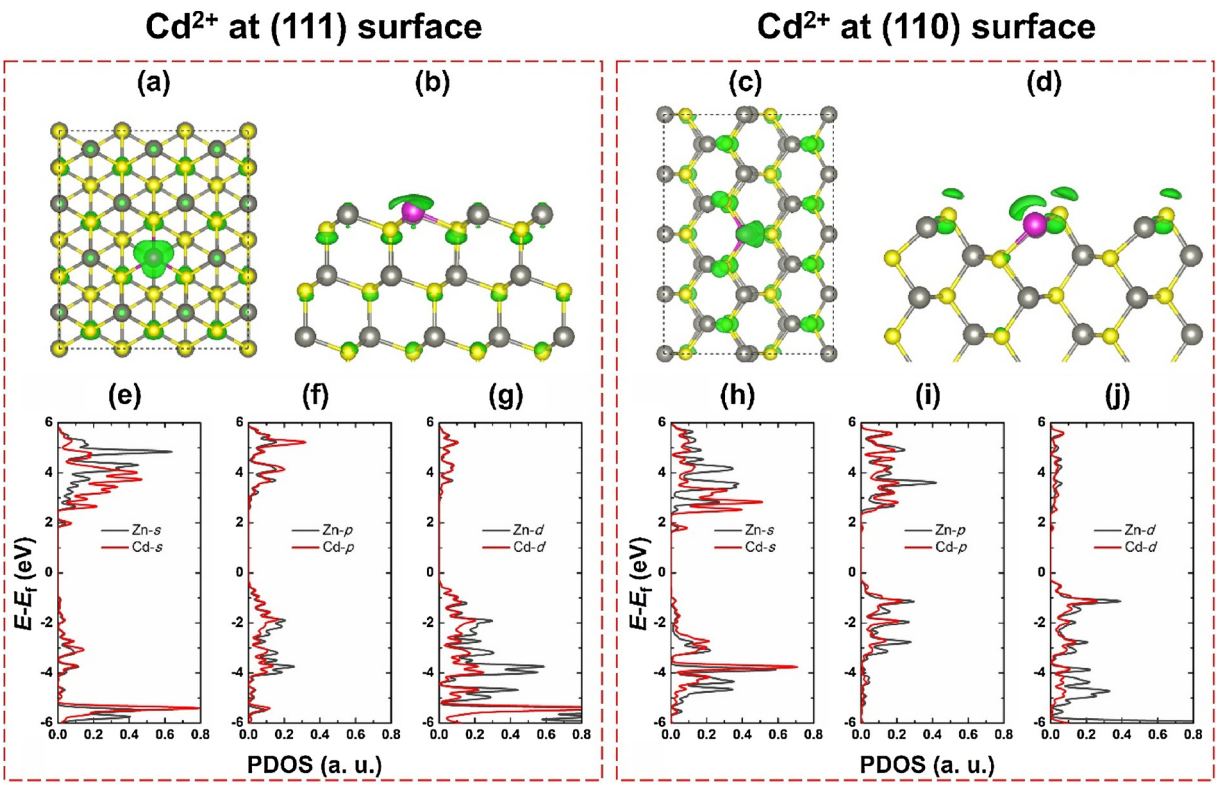

Fig. 5. Charge density distribution of Cd^{2+} modified ZnS (111) and (110) planes from top view (a) and (c), and side view (b) and (d). The gray, yellow and purple balls indicate the Zn, S and Cd atoms, respectively. And the passive H atoms in (111) are not shown here. The green dot surface represents the isosurface of charge density with value of 4×10^{-3} e/Å. (e–j) show the PDOSs of *s*, *p*, and *d* orbitals for Zn and Cd at ZnS (111) and (110) planes, respectively.

higher density of states near band-edge with a relatively lower lying band center than that of Zn *s* orbital (Fig. 5e, h). This reveals that Cd *s* orbital plays the key role in separating electrons from CB of ZnS and catalyzing CO_2 reduction successively. This can be also reasonably understood that the outmost *s* orbital of Cd atom will supply electrons to the electrophilic C atom of CO_2 molecule in the reduction reaction.

3. Conclusion

We have developed Cd/ZnS:Cu nanocrystal photocatalyst for efficient photocatalytic CO_2 reduction under solar light. The rationally-designed Cd/ZnS:Cu nanocrystals take both the solar light harvest and CO_2 reduction kinetics into consideration through Cu doping and Cd grafting, respectively. It is believed that the lower lying Cd *s* orbital electronic state relative to the CB of ZnS and its high PDOS are responsible for the high CO_2 reduction reaction rate and high HCOOH selectivity. It should be highlighted that Cd/ZnS:Cu possibly represents one of the most active and optimized design of sulfide photocatalysts so far for photocatalytic CO_2 reduction under solar light. Cd/ZnS:Cu as well as the all-inorganic reaction system displays many advantages over the other photocatalysts or reaction systems, including i) high CB potential of photocatalyst (thermodynamic requirement), ii) efficient CO_2 reduction selective cocatalyst (kinetic requirement), iii) much better solar light absorption compared with bare colloidal ZnS, iv) noble metal and organic medium free, and v) extreme convenience in material preparation and photocatalytic reaction procedures. Compared with ZnS:Cu, the other potential constituent elements (such as Ag, Ga, and In) of sulfide photocatalysts are difficult to be prepared by heating-free method to design active sulfide photocatalysts [5]. Moreover, for the experimental study, it is also favorable that a sulfide photocatalyst can be operated in an aqueous reaction medium without S^{2-} electron donor during photocatalytic CO_2 reduction because the volatilize H_2S (from the hydrolysis of S^{2-}) will severely deactivate the catalyst fixed inside the commercial methanizer of gas chromatograph based on flame ionization detector (FID), taking serious problem for the gas product analysis. Due to aforementioned advantages, Cd/ZnS:Cu or ZnS:Cu can be used as an ideal model catalysts for the studies related to photocatalytic CO_2 reduction in future. For examples, they can be also used to couple functional organic complexes or inorganic cocatalysts for efficient CO_2 reduction with diversified selectivity, or combine with oxygen evolution photocatalysts to construct Z-scheme system for a CO_2 reduction process with H_2O as reductant, etc.

Acknowledgements

This work received financial support from the National Natural Science Foundation of China (21703065, 21633004, and 51502075), Natural Science Foundation of Hebei Province (B2018209267), World Premier International Research Center Initiative (WPI Initiative) on Materials Nanoarchitectonics (MANA), MEXT, Japan, the National Basic Research Program of China (973 Program, 2014CB239301).

Appendix A. Supplementary data

Supplementary material related to this article can be found, in the online version, at doi:https://doi.org/10.1016/j.apcatb.2018.05.066.

References

[1] R. Kuriki, H. Matsunaga, T. Nakashima, K. Wada, A. Yamakata, O. Ishitani, K. Maeda, J. Am. Chem. Soc. 138 (2016) 5159–5170.
[2] K. Sekizawa, K. Maeda, K. Domen, K. Koike, O. Ishitani, J. Am. Chem. Soc. 135 (2013) 4596–4599.
[3] Y. Kou, Y. Nabetani, D. Masui, T. Shimada, S. Takagi, H. Tachibana, H. Inoue, J. Am. Chem. Soc. 136 (2014) 6021–6030.
[4] X. Meng, Q. Yu, G. Liu, L. Shi, G. Zhao, H. Liu, P. Li, K. Chang, T. Kako, J. Ye, Nano Energy 34 (2017) 524–532.
[5] A. Kudo, Y. Miseki, Chem. Soc. Rev. 38 (2009) 253–278.

[6] A. Kudo, M. Sekizawa, Catal. Lett. 58 (1999) 241–243.
[7] Z. Mei, B. Zhang, J. Zheng, S. Yuan, Z. Zhuo, X. Meng, Z. Chen, K. Amine, W. Yang, L.W. Wang, W. Wang, S. Wang, Q. Gong, J. Li, F.S. Liu, F. Pan, Nano Energy 26 (2016) 405–416.
[8] B.-J. Liu, T. Torimoto, H. Yoneyama, J. Photochem. Photobiol. A: Chem. 113 (1998) 93–97.
[9] H. Li, C. Tsai, A.L. Koh, L. Cai, A.W. Contryman, A.H. Fragapane, J. Zhao, H.S. Han, H.C. Manoharan, F. Abild-Pedersen, J.K. Norskov, X. Zheng, Nat. Mater. 15 (2016) 48–53.
[10] H. Fujiwara, H. Hosokawa, K. Murakoshi, Y. Wada, S. Yanagida, Langmuir 14 (1998) 5154–5159.